

# Robust Heterogeneous Nickel Catalysts with Tailored Porosity for the Selective Hydrogenolysis of Aryl Ethers

Muhammad Zaheer,<sup>[a]</sup> Justus Hermannsdörfer,<sup>[a]</sup> Winfried P. Kretschmer,<sup>[a]</sup> Günter Motz,<sup>[b]</sup> and Rhett Kempe<sup>\*[a]</sup>

**Abstract:** SiC materials with tailored porosity and integrated Ni NPs (Ni@SiC) were synthesized *via* microphase separation of polycarbosilane-*block*-polyethylene followed by its pyrolysis. Changing the length of organic block allowed the synthesis of micro, meso and hierarchical Ni@SiC materials which were characterized by PXRD, TEM, TGA, and nitrogen physisorption. Selective hydrogenolysis of aryl ethers mimicking the most abundant linkages of lignin was achieved in water avoiding the possible hydrogenation of aromatic rings.

The sustainable production of fine chemicals and fuels from renewable resources is a burgeoning and challenging research area.<sup>[1]</sup> Lignocellulose biomass (cellulose, hemi-cellulose and lignin) is a key resource whose availability is plentiful and its utilisation will allay the fears regarding competition with food supplies.<sup>[1,2]</sup> Although cellulose can be depolymerised in many ways,<sup>[3]</sup> selective cleavage of aryl ether (C<sub>Ar</sub>–O) and especially diaryl ether substructures of lignin is challenging.<sup>[4]</sup> Lignin constitutes 15–30% of woody biomass<sup>[5]</sup> with an energy content of up to 40% of this biomass<sup>[6]</sup> and its selective depolymerisation (through hydrogenolysis) is crucial for the generation of fuel and chemicals from renewable resources. Selective cleavage of the C<sub>Ar</sub>–O bond of lignin model compounds in organic solvents has been reported by the use of molecular catalysts (V,<sup>[7]</sup> Ru<sup>[8]</sup> and Ni<sup>[9]</sup> complexes) and heterogeneous catalysts (Ni<sup>[10]</sup> and Zn/Pd<sup>[11]</sup>). The molecular catalysts offer better chemoselectivity in the selective cleavage of C<sub>Ar</sub>–O bonds and are operative under mild conditions (80–135 °C). Unfortunately, they are mostly sensitive to high concentrations of water, the removal of which from the crude biomass is challenging and uneconomical. Heterogeneous catalysts, on the other hand, are not very selective and require higher reaction temperatures or hydrogen pressures, leading to the reduction of arenes and subsequent hydrogen loss. The Lercher group has reported some elegant work on the use of heterogeneous catalysts for

the cleavage of ethers in water.<sup>[12–14]</sup> The substantial reduction of arenes was also observed. Reports on the reusability of the hitherto applied catalysts are rare. Thus, there is a need for reusable catalysts offering hydrothermal stability for the selective cleavage of C<sub>Ar</sub>–O bonds.


In the past few years, others and ourselves have developed late transition metal-containing polymer-derived SiCN materials (M@SiCN) as robust heterogeneous catalysts.<sup>[15]</sup> The Wiesner group fabricated Pt@SiCN materials which, despite the structural control over multiple length scales, showed a rather low surface area.<sup>[16]</sup> By the controlled pyrolysis of Ni modified polysilazane, we managed to get microporous high surface area materials. They were found to be selective and active catalysts for the semi-hydrogenation of acetylenes.<sup>[17]</sup> Unfortunately, the Si–N bonds of the materials pyrolysed at 600 °C were under harsh conditions. SiC materials do not contain such bonds and should offer additional hydrothermal stability. Commercially available silicon carbide possesses low surface area, which limits the effective transport of substances through it for efficient catalysis.<sup>[18]</sup> Self-assembly of block copolymers<sup>[19]</sup> has been applied to the fabrication of mesoporous SiC materials by Kim and co-workers and allows fine tuning of pore morphology.<sup>[20]</sup> Porous iron containing SiC materials have been fabricated by the Manners group through the self-assembly of metal-containing block copolymers.<sup>[21]</sup>

Herein, we report on the synthesis of porous SiC composites with integrated nickel nanoparticles (Ni NPs) starting from organic–inorganic block copolymers. The synthesis, cross-linking and microphase separation of the block copolymers is achieved in a concerted process<sup>[22]</sup> followed by controlled pyrolysis that leads to porous Ni@SiC composite materials. The porosity of the materials can be tailored from micro- to meso-scale including hierarchical (micro–meso) pore structures by changing the molecular weight of the organic block. In particular, the synthesis of mesoporous Ni@SiC materials with an average pore diameter of 4–5 nm is achieved, which is challenging owing to high Laplace pressure leading to pore collapse.<sup>[22]</sup> Phenethoxybenzene (PEB) and diphenylether (DPE), which mimic the most frequent linkages of lignin [ $\beta$ -O-4 (45–62%) and 4-O-5 (4–9%), see Figure 1], are used as model compounds for the chemoselective cleavage of C<sub>Ar</sub>–O bond. The Ni@SiC catalysts are active under mild reaction conditions (90–120 °C, 6 bar hydrogen; 1 bar = 100 kPa) in water providing high selectivity for hydrogenolysis of the C<sub>Ar</sub>–O bond and reusability.

The synthesis of Ni@SiC materials is summarised in Scheme 1. An organic–inorganic block copolymer is formed by

[a] M. Zaheer, J. Hermannsdörfer, Dr. W. P. Kretschmer, Prof. Dr. R. Kempe  
Lehrstuhl Anorganische Chemie II  
Universität Bayreuth  
95440 Bayreuth (Germany)  
E-mail: kempe@uni-bayreuth.de

[b] Dr. G. Motz  
Lehrstuhl Keramische Werkstoffe  
Universität Bayreuth  
95447 Bayreuth (Germany)

 Supporting information for this article is available on the WWW under  
<http://dx.doi.org/10.1002/cctc.201300763>.

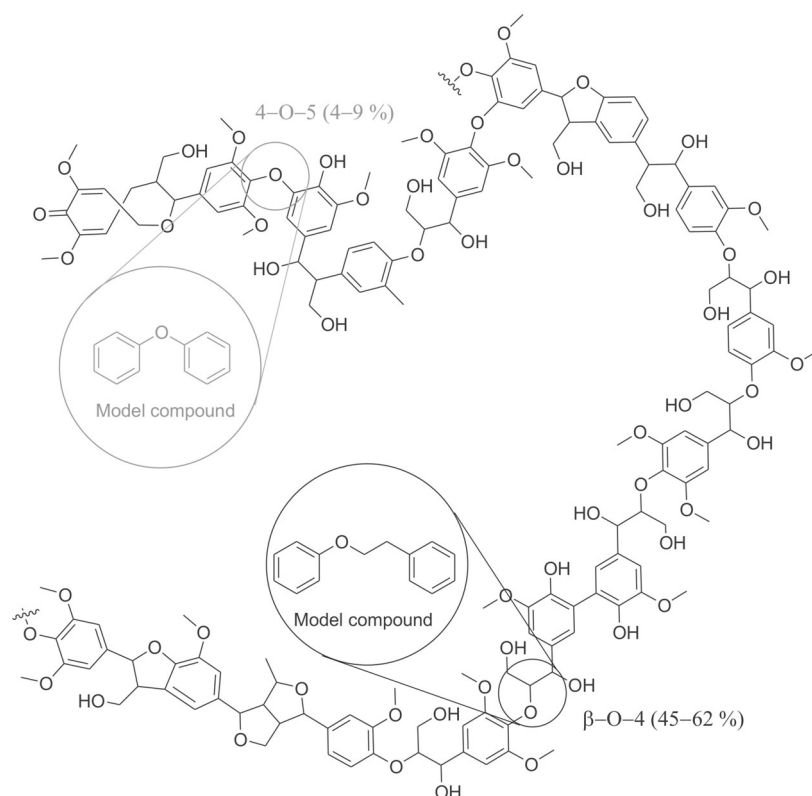
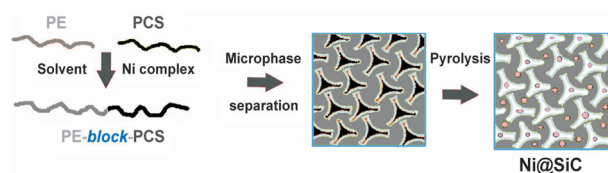


Figure 1. A fragment of hardwood lignin.



Scheme 1. The synthesis of porous Ni@SiC materials through the self-assembly of PCS-*block*-PE. The block copolymer is synthesised through Ni complex-catalysed dehydrocoupling of PCS with PE.

the reaction of the commercially available polycarbosilane (PCS) SMP-10 (Starfire Systems) with hydroxy-terminated polyethylene (PE) through nickel-catalysed dehydrocoupling of Si–H and O–H functions.<sup>[23]</sup> As both blocks are immiscible and covalently linked, the microphases separate into microdomains, providing a nanostructured material. The PE block used is inexpensive and can be produced efficiently by using molecular catalysts.<sup>[24]</sup> The crystallisation behaviour of strictly linear PE allows good morphology control even in combination with rather ill-defined inorganic blocks.<sup>[25]</sup> The added nickel complex ( $[\text{Ni}(\text{Ap})_2]_2$  where  $\text{Ap-H} = 4\text{-methyl-2-}((\text{trimethylsilyl})\text{amino})\text{pyridine}$ , see Figure S1 in the Supporting Information for its structure) also catalyses the cross-linking of the PCS block, for example, through homocoupling of the Si–H bonds. The organic block is burnt out during pyrolysis ( $700^\circ\text{C}$  in Ar), whereas  $\text{Ni}^{\text{II}}$  species are reduced to elemental nickel. Thus, porous SiC materials with integrated Ni NPs are generated. The loading of the nickel complex is adjusted such that the final materials

after pyrolysis contain 4.3 wt% of nickel (Si/Ni atomic ratio  $\approx 20:1$ , Table S2). The molecular weight of the organic block (PE) affects the type of porosity generated in the Ni@SiC catalyst. The use of PE with a molecular weight of  $1740\text{ g mol}^{-1}$  provides a mesoporous Ni@SiC material after self-assembly and pyrolysis. The material, as investigated by TEM, shows Ni NPs with an average size of 3.3 nm (Figure 2c). The nitrogen adsorption–desorption isotherm as presented in Figure 2e is typical for a mesoporous material. The closure of the desorption branch at a relative pressure of  $\approx 0.4$  owes to capillary condensation, a characteristic process known for mesopores. To a BET surface area ( $S_{\text{BET}}$ ) of  $450\text{ m}^2\text{ g}^{-1}$ , only  $38\text{ m}^2\text{ g}^{-1}$  is contributed by micropores, as calculated by t-plot method (Table S3, entry 1). The size of the pores is calculated by non-localised DFT (adsorption branch) and is in the 2–8 nm size range (Figure 2f).

The presence of Ni NPs (cubic nickel, ICDD PDF number: 00-001-1260) was confirmed by powder X-ray diffraction (PXRD, see Figure 2d). If the molecular weight of the organic block (PE) is decreased to  $326\text{ g mol}^{-1}$ , microporous materials ( $S_{\text{BET}} = 552\text{ m}^2\text{ g}^{-1}$ ) are obtained. The material shows a typical type-I adsorption isotherm (Figure 3c) with an average pore width of 1.3 nm (Figure S6). The specific surface area shows a small contribution ( $69\text{ m}^2\text{ g}^{-1}$ ) from mesopores (Table S3, entry 2). The Ni NPs are smaller in size (mean diameter = 2.4 nm, Figure 3b) than the mesoporous materials and are uniformly distributed over the material (Figure 3a). The PXRD pattern of the material (Figure S7a) confirms the presence of Ni NPs. At this stage, it seems that porosity of the Ni@SiC materials can be tailored by varying the molecular weight of PE. Lower molecular weight PE ( $326\text{ g mol}^{-1}$ ) provides microporous materials, whereas mesoporous materials can be obtained by higher molecular weight PE ( $1740\text{ g mol}^{-1}$ ). We thus expected to obtain a hierarchically structured material (micro- and mesopores) by the use of PE with intermediate chain lengths. If PE with a molecular weight of  $550\text{ g mol}^{-1}$  was used, composites with hierarchical porosity (SiC-hier) were obtained. The formation of amorphous SiC was confirmed by FTIR and solid state  $^{29}\text{Si}$  NMR analysis of the materials (Figure S8). The latter shows broad peaks at  $-16$  and  $-65$  ppm assigned to  $\text{SiC}_4$  and  $\text{CSiO}_3$  environments, respectively.<sup>[26]</sup> A slight amount of oxygen in the materials comes from the hydroxy-terminated PE. As shown in Figure 3d, these materials contain nickel nanoparticles with an average size of 2.7 nm. High uptake of nitrogen both at lower and higher rela-

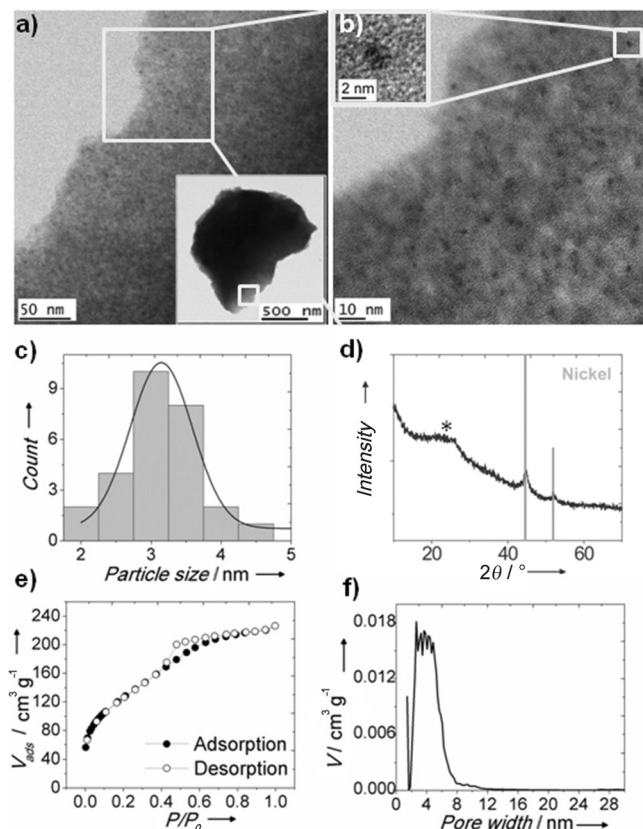


**Figure 2.** a, b) TEM micrographs of mesoporous Ni@SiC (SiC-meso) and c) the corresponding Ni particle size distribution. d) PXRD pattern with nickel reflexes and asterisk denoting graphitic phases. The carbon phase forms as a result of considerable polyethylene cracking during pyrolysis. e) Nitrogen adsorption-desorption isotherm and f) the corresponding pore size distribution, calculated by using a non-localised DFT model with silica kernels of cylindrical pore geometry.

tive pressure values (Figure 3 e) is indicative of the existence of both micro- and mesopores. The non-localised DFT model applied to the nitrogen adsorption isotherm (Figure 3 f) confirms the existence of micro- and mesopores. Contributions to the total surface area of SiC-hier (527 m<sup>2</sup> g<sup>-1</sup>) came partly from the micropores (326 m<sup>2</sup> g<sup>-1</sup>) and partly from the mesopores (202 m<sup>2</sup> g<sup>-1</sup>), as tabulated in Table S3. The pores were generated because of gaseous emissions (mostly cracked hydrocarbons) from the organic block during pyrolysis (see Figure S9 for thermogravimetric analyses of all materials). Mass losses (300–500 °C) are in accordance with the loss of the PE block during pyrolysis.

The selective hydrogenolysis of lignin model compounds was studied in water under 6 bar hydrogen pressure. Comparison of the activities of all three types of Ni@SiC materials was tested in the hydrogenolysis of benzyl phenyl ether at 110 °C for 20 h (Table 1). SiC-hier was found to be the most active catalyst providing 99% conversion (entry 1). In case of microporous SiC-micro, a conversion of 75% was observed (entry 2) under the same conditions. Mesoporous Ni@SiC (SiC-meso) showed only 26% conversion (entry 3). The selectivity towards aromatic products (phenol and toluene) was high in all experiments. As aryl ethers are insoluble in water, the addition of

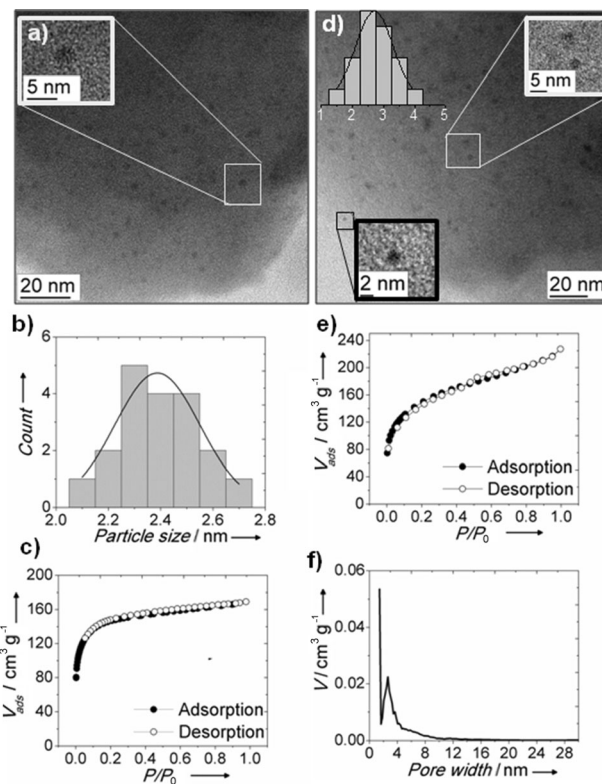


**Figure 3.** a) TEM micrograph with a high resolution inset, b) Ni particle size distribution and c) nitrogen adsorption isotherm of the SiC-micro material. d) TEM micrograph with Ni particle size count and high resolution insets, e) nitrogen adsorption isotherm and f) pore size distribution calculated by using a non-localised DFT model of the SiC-hier material.

a TBAB (tetra-*n*-butylammonium bromide) could be advantageous. With the addition of 0.3 equivalents of TBAB, hydrogenolysis of benzyl phenyl ether was achieved even at 90 °C.

**Table 1.** Hydrogenolysis of benzyl phenyl ether with Ni@SiC.<sup>[a]</sup>

Entry	Catalyst	<i>T</i> [°C]	KOtBu [equiv.]	TBAB [equiv.]	Conv. [%] (TON) <sup>[c]</sup>	Sel. <sup>[d]</sup> [mol %]
1	SiC-hier <sup>[b]</sup>	110	–	–	99 (16)	81
2	SiC-micro <sup>[b]</sup>	110	–	–	75 (12)	94
3	SiC-meso <sup>[b]</sup>	110	–	–	26 (4)	98
4	SiC-micro	90	1	0.3	90 (38)	99
5	SiC-hier	90	1	0.3	99 (42)	99
6	SiC-meso	90	1	0.3	64 (27)	99

[a] Conditions: 0.5 mmol of ether was mixed with 15 mg of catalyst (1.17 × 10<sup>-5</sup> mol Ni) in 2 mL H<sub>2</sub>O at a H<sub>2</sub> pressure of 6 bar and stirred (1000 rpm) at a specified temperature for 20 h. [b] 40 mg catalyst (3.13 × 10<sup>-5</sup> mol Ni) and a H<sub>2</sub> pressure of 10 bar was used. [c] Turnover numbers were calculated based on the total amount of Ni in the materials. [d] Selectivity to phenol.

Again, SiC-hier showed the highest activity (entry 5) compared with SiC-micro (90%, entry 4) and SiC-meso (64%, entry 6). The higher activity of SiC-hier could have resulted from the better accessibility of catalytically active nickel NPs in the hierarchically porous material. At this temperature, no further hydrogenation of phenol to cyclohexanol was observed, providing phenol in 99% selectivity.

SiC-hier, owing to its higher activity than the other two catalysts (SiC-micro and SiC-meso), was chosen for the selective cleavage of the  $\beta$ -O-4 linkage to phenol and ethylbenzene (Table 2). No conversion was observed at 120 °C in the absence

ether, after which it remained almost constant (see Figure S11 a). Keeping the amount of TBAB at 0.3 equivalents, increasing the concentration of NaOtBu base increased the overall conversion up to 1 equivalent of base relative to the ether. With more than 1 equivalent of base, the conversion decreased (see Figure S11 b). These optimised conditions were also applied to selectively cleave DPE, the model compound for the 4-O-5 linkage (Figure 1). 50% of DPE was converted into phenol and benzene by using SiC-hier (entry 10). The phenol selectivity was nearly quantitative. By doubling the catalyst loading and increasing the amounts of base and phase-transfer catalyst, an almost quantitative conversion of DPE was achieved within 20 h (entry 11). The selectivity towards phenol and benzene was again as high as 97%. These results showed the hierarchical Ni@SiC materials to be highly selective towards hydrogenolysis of the C–O bond of DPE without hydrogenation of the aromatic ring(s). In comparison to previous works, we have achieved the selective cleavage of C–O bonds in water (avoiding the use of organic solvents) and with a lower nickel content (4.3 wt%). The recycling of the catalyst SiC-hier was tested with almost 50% conversion at 120 °C under 6 bar of hydrogen. No prominent loss in the activity was observed after up to five consecutive catalytic runs (see Figure S12).

In summary, we have synthesised robust porous SiC materials with integrated Ni nanoparticles. Porosity was achieved through the self-assembly of organic–inorganic block copolymers. Depending upon the molecular weight of the organic block (inexpensive polyethylene), the fabrication of micro-, meso- and hierarchically porous Ni@SiC catalysts was possible. All catalysts were found to be active and highly selective in ether hydrogenolysis. The hierarchically structured Ni@SiC material was the most active catalyst. It was reusable and highly selective towards the hydrogenolysis of diphenylether, a challenging lignin model compound.

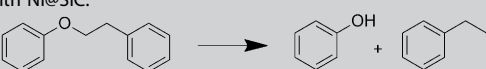

## Experimental Section

The starting materials 4-methyl-2-((trimethylsilyl)amino)pyridine (Ap-H),<sup>[27]</sup> Ni complex  $[\text{Ni}(\text{Ap})_2]_2$ <sup>[28]</sup> and phenethoxybenzene<sup>[13a]</sup> were synthesised by following reported methods.

SiC-micro and SiC-hier Ni@SiC materials were fabricated by the reaction of PE-326 and PE-550 with PCS in THF, respectively. In a vial placed in a Schlenk tube, PE (1 g) was dissolved in THF (8 mL), followed by the addition of PCS (1 g) and Ni complex  $[\text{Ni}(\text{Ap})_2]_2$  (0.400 g,  $4.79 \times 10^{-4}$  mol, Ni/Si = 1:20). The solution was annealed at 80 °C for 24 h, during which the solvent came out of the vial into the Schlenk tube. Finally, the solid was cooled slowly to RT.

For the synthesis of SiC-meso materials, PCS SMP-10 (1 g) and PE-1739 (1 g) were dissolved in cumene (10 mL) at 150 °C. Afterwards, a solution of the Ni complex  $[\text{Ni}(\text{Ap})_2]_2$  (0.400 g,  $4.91 \times 10^{-4}$  mol) in cumene (7 mL) was added. The mixture was cooled to 140 °C and annealed at this temperature for 24 h. Lastly, the obtained solid was slowly cooled to RT and traces of the solvent were removed under vacuum.

The catalytic selective hydrogenolysis of lignin model compounds was done in a Parr autoclave under a  $\text{H}_2$  pressure of 6–10 bar. A glass tube was charged with a magnetic stirrer bar and milled cata-

<b>Table 2.</b> Hydrogenolysis of phenethoxybenzene (entries 1–9) and DPE (entries 10–11) with Ni@SiC. <sup>[a]</sup>						
						
						
Entry	Catalyst	Base [equiv.]	TBAB [equiv.]	Conv. [%] (TON)	Sel. <sup>[b]</sup> [%]	
1	SiC-hier	–	–	0	0	
2	SiC-hier	–	0.3	0	0	
3	SiC-hier	NaOH (1)	–	27	99	
4	SiC-hier	NaOH (1)	0.3	93	92	
5	SiC-hier	K <sub>2</sub> CO <sub>3</sub> (1)	0.3	71	84	
6	SiC-hier	NaOtBu (1)	0.3	89	94	
7	SiC-hier	KOtBu (1)	0.3	99 (42)	96	
8	SiC-micro	NaOH (1)	0.3	78 (33)	95	
9	SiC-meso	NaOH (1)	0.3	25 (11)	99	
10	SiC-hier	KOtBu (1)	0.3	50	98	
11	SiC-hier <sup>[c]</sup>	KOtBu (2.5)	1.0	96 (14)	97	

[a] Conditions: 0.5 mmol of ether was mixed with 15 mg of catalyst ( $1.17 \times 10^{-5}$  mol Ni) in 2 mL H<sub>2</sub>O at a H<sub>2</sub> pressure of 6 bar and then stirred (1000 rpm) at 120 °C for 20 h. [b] Selectivity to phenol (ethylbenzene/benzene selectivity > 99% in all cases). Turnover numbers were calculated based on the total amount of Ni in the materials. [c] 30 mg Catalyst was used ( $3.42 \times 10^{-5}$  mol Ni).

of base and TBAB (entry 1) or in the presence of TBAB alone (entry 2). A minor conversion (27%) was achieved by the addition of a base (entry 3), which increased greatly (93%) upon addition of both base and TBAB (entry 4). Addition of TBAB would have improved the solubility of aryl ethers in water, whereas the base promoted the cleavage of C–O bonds, as previously documented.<sup>[10b]</sup> Whereas lower conversion and selectivity was obtained by using K<sub>2</sub>CO<sub>3</sub> as a base (entry 5), NaOtBu and KOtBu provided good yields and selectivities (entries 6–7).

In comparison to SiC-hier, the other two materials (SiC-micro and SiC-meso) had lower activities (entries 8–9). A minor conversion of phenol to cyclohexanol (hydrogenation product of phenol) was observed in all cases, indicating a high chemoselectivity of hydrogenolysis over hydrogenation provided by the catalysts. The effect of the amount of TBAB and base was also investigated. On increasing the amount of TBAB, conversion increased with up to of 0.3 equivalents of TBAB relative to the



lyst (particle size < 100  $\mu\text{m}$ ) and placed in the reactor, which was then filled with  $\text{H}_2$  at RT. The reactor was heated to the respective temperature (90, 110, or 120  $^\circ\text{C}$ ) within 20 min and stirring was continued at this temperature for 20 h. Afterwards, dodecane was added and mixture was extracted with ethyl acetate (3  $\times$  2 mL). The conversion and selectivity were determined by GC.

For the reusability studies, the catalyst was washed with EtOH and  $\text{H}_2\text{O}$  and dried at 80  $^\circ\text{C}$  under vacuum.

## Acknowledgements

This work was financially supported by the Deutsche Forschungsgemeinschaft, SFB 840. Authors are thankful to Bernard Putz for PXRD analysis. Dr. Caroline D. Keenan, Dr. Yamini S. Avadhut and Prof. Dr. Jürgen Senker are acknowledged for the solid-state NMR measurements and discussions. Muhammad Zaheer expresses his gratitude to HEC Pakistan and DAAD for the fellowship.

**Keywords:** hydrogenolysis • lignin • nickel • nanoparticles • sustainable chemistry

- [1] C. O. Tuck, E. Perez, I. T. Horvath, R. A. Shelden, M. Poliakoff, *Science* **2012**, 337, 695–699.
- [2] a) C. H. Zhou, X. Xia, C. X. Lin, D. S. Tong, J. Beltrami, *Chem. Soc. Rev.* **2011**, 40, 5588–5617; b) P. Gallezot, *Chem. Soc. Rev.* **2012**, 41, 1538–1558; c) M. Alonso, S. G. Wettstein, J. A. Dumesic, *Chem. Soc. Rev.* **2012**, 41, 8075–8098; d) R. Rinaldi, F. Schueth, *Energy Environ. Sci.* **2009**, 2, 610–626; e) Y. C. Lin, G. W. Huber, *Energy Environ. Sci.* **2009**, 2, 68–80; f) J. Q. Bond, D. M. Alonso, D. Wang, R. M. West, J. A. Dumesic, *Science* **2010**, 327, 1110–1114; g) Y. Román-Leshkov, C. J. Barret, Z. Y. Liu, J. A. Dumesic, *Nature* **2007**, 447, 982–986; h) P. Anbarasan, Z. C. Baer, S. Sreekumar, E. Gross, J. B. Binder, H. W. Blanch, D. S. Clark, F. D. Toste, *Nature* **2012**, 491, 235–239.
- [3] a) A. Corma, S. Iborra, A. Velty, *Chem. Rev.* **2007**, 107, 2411–2502; b) G. W. Huber, S. Iborra, A. Corma, *Chem. Rev.* **2006**, 106, 4044–4098.
- [4] a) E. Furimsky, *Appl. Catal. A* **2000**, 199, 147–190; b) J. Z. Pieter, C. A. Bruijninx, A. L. Jongerius, B. M. Weckhuysen, *Chem. Rev.* **2010**, 110, 3552–3599.
- [5] M. Stöcker, *Angew. Chem.* **2008**, 120, 9340–9351; *Angew. Chem. Int. Ed.* **2008**, 47, 9200–9211.
- [6] J. R. Regalbuto, *Science* **2009**, 325, 822–824.
- [7] S. Son, F. D. Toste, *Angew. Chem.* **2010**, 122, 3879–3882; *Angew. Chem. Int. Ed.* **2010**, 49, 3791–3794.
- [8] J. M. Nichols, L. M. Bishop, R. G. Bergman, J. A. Ellman, *J. Am. Chem. Soc.* **2010**, 132, 12554–12555.
- [9] a) A. G. Sergeev, J. F. Hartwig, *Science* **2011**, 332, 439–443; b) M. Tobisu, K. Yamakawa, T. Shimasaki, N. Chatani, *Chem. Commun.* **2011**, 47, 2946–2948; c) B. S. Samant, G. W. Kabalka, *Chem. Commun.* **2012**, 48, 8658–8660.
- [10] a) X. Wang, R. Rinaldo, *ChemSusChem* **2012**, 5, 1455–1466; b) A. G. Sergeev, J. D. Webb, J. F. Hartwig, *J. Am. Chem. Soc.* **2012**, 134, 20226–20229; c) E. M. Van-Duzee, H. Adkins, *J. Am. Chem. Soc.* **1935**, 57, 147–151.
- [11] T. H. Parsell, B. C. Owen, I. Klein, T. M. Jarrell, C. L. Marcum, L. J. Hauptert, L. M. Amundson, H. I. Kenttämä, F. Ribeiro, J. T. Miller, M. M. Abu-Omar, *Chem. Sci.* **2013**, 4, 806–813.
- [12] V. M. Roberts, R. T. Knapp, X. Li, J. A. Lercher, *ChemCatChem* **2010**, 2, 1407–1410.
- [13] a) C. Zhao, J. A. Lercher, *Angew. Chem.* **2012**, 124, 6037–6042; *Angew. Chem. Int. Ed.* **2012**, 51, 5935–5941; b) C. Zhao, J. A. Lercher, *ChemCatChem* **2012**, 4, 64–68.
- [14] J. He, C. Zhao, J. A. Lercher, *J. Am. Chem. Soc.* **2012**, 134, 20768–20775.
- [15] a) G. Glatz, T. Schmalz, T. Kraus, F. Haarmann, G. Motz, R. Kempe, *Chem. Eur. J.* **2010**, 16, 4231–4238; b) M. Zaheer, G. Motz, R. Kempe, *J. Mater. Chem.* **2011**, 21, 18825–18831; c) T. Schmalz, T. Kraus, M. Guenther, C. Liebscher, U. Glatzel, R. Kempe, G. Motz, *Carbon* **2011**, 49, 3065–3072; d) M. Zaheer, T. Schmalz, G. Motz, R. Kempe, *Chem. Soc. Rev.* **2012**, 41, 5102–5116.
- [16] M. Kamperman, A. Burns, R. Weissgraeber, N. van Vegten, S. C. Warren, S. M. Gruner, A. Baiker, U. Wiesner, *Nano Lett.* **2009**, 9, 2756–2762.
- [17] M. Zaheer, C. D. Keenan, J. Hermannsdörfer, E. Roessler, G. Motz, J. Senker, R. Kempe, *Chem. Mater.* **2012**, 24, 3952–3963.
- [18] Y. Shi, Y. Wan, D. Zhao, *Chem. Soc. Rev.* **2011**, 40, 3854–3878.
- [19] Y. Mai, A. Eisenberg, *Chem. Soc. Rev.* **2012**, 41, 5969–5985.
- [20] a) Q. D. Nghiem, D. P. Kim, *Chem. Mater.* **2008**, 20, 3735–3739; b) Q. D. Nghiem, D. P. Kim, S. O. Kim, *J. Nanosci. Nanotechnol.* **2008**, 8, 5527–5531.
- [21] a) D. A. Rider, K. Liu, J. C. Eloi, L. Vanderark, L. Yang, J. Y. Wang, D. Grozea, Z. H. Lu, T. R. Russel, I. Manners, *ACS Nano* **2008**, 2, 263–270; b) K. Temple, K. Kulbaba, K. N. Power-Billard, I. Manners, K. A. Leach, T. Xu, T. M. Russel, C. J. Hawker, *Adv. Mater.* **2003**, 15, 297–300.
- [22] M. Seo, M. A. Hillmyer, *Science* **2012**, 336, 1422–1425.
- [23] a) B. H. Kim, M. S. Cho, M. A. Kim, H. G. Woo, *J. Organomet. Chem.* **2003**, 685, 93–98; b) B. H. Kim, M. S. Cho, H. G. Woo, *Synlett* **2004**, 761–772; c) E. Lukevics, M. Dzintara, *J. Organomet. Chem.* **1985**, 295, 265–315.
- [24] S. T. K. Pillai, W. P. Kretschmer, M. Trebbin, S. Förster, R. Kempe, *Chem. Eur. J.* **2012**, 18, 13974–13978.
- [25] S. K. T. Pillai, W. P. Kretschmer, C. Denner, G. Motz, M. Hund, A. Fery, M. Trebbin, S. Förster, R. Kempe, *Small* **2013**, 9, 984–989.
- [26] a) T. Taki, M. Inui, K. Okamura, M. Sato, *J. Mater. Sci. Lett.* **1989**, 8, 918–920; b) C. Hoffmann, T. Biemelt, A. Seifert, K. Pinkert, T. Gemming, S. Spange, S. Kaskel, *J. Mater. Chem.* **2012**, 22, 24841–24847; c) Q. Liu, H. J. Wu, R. Lewis, G. E. Maciel, L. V. Interrante, *Chem. Mater.* **1999**, 11, 2038–2048.
- [27] R. Kempe, P. Arndt, *Inorg. Chem.* **1996**, 35, 2644–2649.
- [28] S. Deeken, S. Proch, E. Casini, H. F. Braun, C. Mechtler, C. Marschner, G. Motz, R. Kempe, *Inorg. Chem.* **2006**, 45, 1871–1879.

Received: September 11, 2013

Published online on October 21, 2013